Magnetoacoustic Tomography with Magnetic Induction: Multiphysics Imaging Approach_A Short Review

Sani Saminu
State Key Laboratory of Reliability and Intelligence of Electrical Equipment Hebei University of Technology Tianjin 300130, China
sansam4k@gmail.com

Guizhi Xu
State Key Laboratory of Reliability and Intelligence of Electrical Equipment Hebei University of Technology Tianjin 300130, China
gzxu@hebut.edu.cn

Shuai Zhang
State Key Laboratory of Reliability and Intelligence of Electrical Equipment Hebei University of Technology
Tianjin 300130, China
zs@hebut.edu.cn

Abd El Kader Isselmou
State Key Laboratory of Reliability and Intelligence of Electrical Equipment Hebei University of Technology
Tianjin 300130, China
isselmou_kader@yahoo.com

Adamu Halilu Jabire
Department of Electrical and Electronics Engineering Taraba Statee University Jalingo, Nigeria
adamu.jabire@tsuniversity.edu.ng

Adamu Ya'u Iliyasu
Advanced RF and Microwave Research Group, School of Electrical Engineering, Faculty of Engineering, Universiti Teknologi Malaysia (UTM), 81310 UTM, Johor Bahru, Malaysia
alhaji080@gmail.com

***Abstract*—Magnetoacoustic tomography with magnetic induction (MAT-MI) is one of the multiphysics imaging techniques that combines the principle of magnetic field excitation and acoustic vibration. It is a noninvasive imaging technique developed in order to achieve high electrical impedance contrast of biological tissue as well as high spatial resolution close to ultrasound imaging. The feasibility to reconstruct high spatial resolution conductivity images using MAT-MI method has been demonstrated by both computer simulation and experimental studies. This work reviews the summary of fundamental ideas of MAT-MI and major techniques developed in recent years. First, the physical mechanisms underlying MAT-MI imaging are described including the magnetic induction and Lorentz force induced acoustic wave propagation. Second, experimental setups and various imaging strategies for MAT-MI are reviewed. Finally, we give our opinions on existing challenges and future directions for MAT-MI research. With all the reported and future technical advancement, MAT-MI has the potential to become an important noninvasive modality for electrical conductivity imaging of biological tissue.**

Keywords—MAT-MI, Multiphysics, Noninvasive Imaging, Biological Tissues, MRI.

[1] INTRODUCTION

Multiphysics problems, which include hybrid imaging techniques have been given great attention and enormous research interest over the years [1,2]. They are called hybrid because they utilize couplings of physical modalities in which the measurement quantities and excitation are belong to different physical modalities [3,4]. Medical imaging techniques are playing increasingly important roles in biomedical research and clinical diagnosis. A number of efforts have been made to improve our ability to characterize tissue properties such as to image the electrical impedance of biological tissues using noninvasive measurements. Also, Electrical properties of biological tissue including electrical conductivity σ and permittivity γ are very important in understanding the interactions and the effects of electromagnetic fields on our body. Also, biophysical parameters in the studies and analysis of electromagnetic therapies like transcranial stimulation methods and electrophysiology reflects the structural, functional and pathological conditions of tissues [5-7]. In addition, tissue electrical properties may serve as an imaging contrast for possible diagnosis and research applications due to their changes under physiological and pathological conditions [8]. They are determined by the molecular composition, cellular structure, amount of intra- and extra-cellular fluids, mobility and concentration of ions, temperature and many other factors. Therefore, measurements of tissue electrical properties could provide valuable information for guidance of neuronal stimulation in neuroscience, radio frequency patient safety in magnetic resonance imaging (MRI), and could be used as a new endogenous biomarker for example in oncology [9-11].

A number of efforts have been made over the decades to developed different hybrid imaging methods in order to characterize tissue properties and to measure electrical properties of biological tissue, which include Electrical Impedance Tomography (EIT) [12,13], magnetic resonance electrical impedance tomography (MREIT) [14,15]. magnetic induction tomography (MIT) [16], and magnetoacoustics tomography (MAT) [17-19]. To addressed the limitations of these proposed methods such as low spatial resolution, degraded sensitivity, and shielding effect as in EIT [20]. Use of MRI machine which makes MREIT more expensive and high level current injection requirement for good SNR value. For MIT, due to ill-posed inverse problem, the spatial resolution of this technique is also limited. Also, for the methods that coupled electromagnetic field and acoustic field such as in MAT and HEI or MAET or LFEIT, the problem of the "shielding effect" associated with the use of surface electrodes for current injection or voltage measurement, i.e. regions surrounded by low-conductive tissue become invisible, still exists in these methods [21-23]. Therefore, MAT-MI has been proposed as an alternative and suitable method to image electrical tissues.

MAT-MI utilizes magnetic induction to induce eddy current in the conductive sample and generates acoustic vibrations through the same Lorentz force coupling mechanism as in MAT or HEI. Ultrasound waves are then

sensed to reconstruct the electrical conductivity related images. Ever since the MAT-MI method was proposed, there have been many numerical studies [24-26] and experimental studies using physical phantoms [27,28] or biological tissues [29-31] demonstrating the feasibility and performance of MAT-MI. Advancement on experimental system design [32,33] and image reconstruction algorithms [34,35] has also been achieved in recent years. In addition, similar to the reverse mode of HEI or MAET, i.e. applying ultrasound transmission and measuring the Lorentz force induced current or voltage for imaging electrical conductivity, the reverse mode of MAT-MI named magneto-acousto-electrical tomography with magnetic induction (MAET-MI) has also been developed recently [36,37], which uses ultrasound stimulation and coil measurement of the dynamic magnetic field generated by Lorentz force induced current in conductive imaging objects.

This report is aim at providing an overview over the basic background concepts of theories and physical principles behind MAT-MI imaging methodology. Also review of numerical, experimental studies during these recent years have been presented. Finally, the report would be concluded with challenges and future direction for technical improvement.

[2] BACKGROUND

As shown in fig 1. the basic principle of MAT-MI is that the conductive object with electrical conductivity σ(r) (where r is the position vector is placed in a static magnetic field B_0 and a time-varying magnetic stimulation with magnetic flux density B_1 is applied to induce eddy current J inside the object volume Ω. the conductivity distribution σ(r) and field B_1 determined the induced current while the system frequency considered is in MHz and the displacement current is much smaller than the conduction current [38], so permittivity which is related to tissue capacitance is neglected. the Lorentz force F described in (1) formed the eddy current by moving charged iron and therefore generates ultra sound pressure signal to be detected by ultra sound probes so that electrical conductivity map of the object's can be estimated.

$$F = J \times B_0 \quad (1)$$

MAT-MI two essentials mechanisms are described as follows [39]:

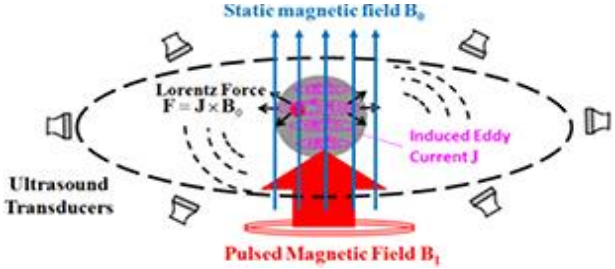


Fig. 1. Basic Principle of MAT-MI

2.1 Magnetic induction in conductive tissue sample

In MAT-MI, the magnetic induction problem can be regarded as quasi-static and by that the spatial and temporal functions of the time-varying magnetic field can be separated, i.e.

$$\mathbf{B_1}(\mathbf{r},t) = \mathbf{B_1}(\mathbf{r})f(t) \quad (2)$$

From (2), it shows that magnetic field in the tissue can be well approximated by the field produced by the coil in the absence of the tissue and can be estimated with the known coil geometry [40].

Using the magnetic vector potential $\mathbf{A}(\mathbf{r},t)$ as $\mathbf{B_1} = \nabla \times \mathbf{A}$. According to Faraday's law, we have

$$\nabla \times \left(E + \frac{\partial A}{\partial t}\right) = 0 \quad (3)$$

where $\mathbf{E}(\mathbf{r}, t)$ is the electrical field intensity. Therefore the electrical field intensity $\mathbf{E}(\mathbf{r},t)$ can be written as:

$$E = -\nabla \emptyset - \frac{\delta A}{\delta t} \quad (4)$$

where $\phi(\mathbf{r}, t)$ is the electrical scalar potential. According to Ampere's law and because we ignore the displacement current, the current density $\mathbf{J}(\mathbf{r},t)$ is solenoidal as:

$$\nabla . \mathbf{J} = 0 \quad (5)$$

In addition, according to Ohm's law, the current density is related to the electrical field through conductivity as:

$$\mathbf{J} = \boldsymbol{\sigma}\mathbf{E} \quad (6)$$

Combining Equations (4)-(6), we can have:

$$\nabla . (\sigma \nabla \emptyset) = -\nabla . \left(\sigma \frac{\delta A}{\delta t}\right) \quad (7)$$

According to the quasi-static condition, Faraday's Law and Ohm's Law, the similar spatial and temporal separation holds for the magnetic vector potential, induced electrical field and eddy current density, i.e. $\mathbf{A}(\mathbf{r},t) = \mathbf{A}(\mathbf{r})f(t)$, $\phi(\mathbf{r},t) = \phi(\mathbf{r})f'(t)$, $\mathbf{E}(\mathbf{r},t) = \mathbf{E}(\mathbf{r})f'(t)$ and $\mathbf{J}(\mathbf{r},t) = \mathbf{J}(\mathbf{r})f'(t)$ where the prime denotes the first order time derivative.

2.2 Lorentz force induced acoustic wave propagation

With magnetically induced eddy current $\mathbf{J}$ and the static magnetic field $\mathbf{B}_0$, the Lorentz force acting on the eddy current over unit volume can be written as

$$\mathbf{F} = \mathbf{J} \times \mathbf{B}_0 \quad (8)$$

Note here that we assumed $B_1 << B_0$ as the strength of the dynamic field for magnetic induction is much smaller than that of the static field in most of the MAT-MI experiment systems. According to Newton's second law of motion and assuming the particle velocity $\mathbf{v}$ caused by the Lorentz force is small as described in Equation (9) [41,42]:

$$\frac{\partial(\rho 0 \boldsymbol{v})}{\partial t} = -\nabla p + \boldsymbol{J} \times \boldsymbol{B_0} \quad (9)$$

where ρ_0 is the density of the material at rest and p is acoustic pressure. Taking the divergence of both sides of (9), we have Equation (10):

$$\frac{\partial(\nabla.(\rho 0 \boldsymbol{v}))}{\partial t} = -\nabla^2 p + \nabla . (\boldsymbol{J} \times \boldsymbol{B_0}) \quad (10)$$

In addition, we have the conservation of mass as in (11) and the definition of the adiabatic compressibility of the medium βs is shown in in Equation (12):

$$\nabla . (\rho 0 \boldsymbol{v}) = -\frac{\partial \rho}{\partial t} \quad (11)$$

$$\beta_s \boldsymbol{p} = \frac{\boldsymbol{\rho}}{\boldsymbol{\rho 0}} \quad (12)$$

where ρ is the density variation. Combining Equations (10)-(12) and using the relationship $C_s = \frac{1}{\sqrt{\rho 0 \beta s}}$where c_s is the acoustic speed in the medium, we can derive the wave

equation with the Lorentz force induced acoustic source [36]:

$$\nabla^2 p - \frac{1}{c_s^2}\frac{\partial^2 p}{\partial t^2} = \nabla.(\boldsymbol{J} \times \boldsymbol{B_0}) \quad (13)$$

Note here that in MAT-MI, the static magnetic field is generally generated from some external sources such as permanent magnets placed outside the imaging object volume, thus $\nabla \times \mathbf{B}0 = 0$ inside the imaging object volume [40,41].

[3] EXPERIMENTAL SETUP

The experimental setup for MAT-MI has three essential components, static magnetic field, dynamic magnetic field, and ultrasound transducer to capture ultrasound signals as shown in fig. 2.

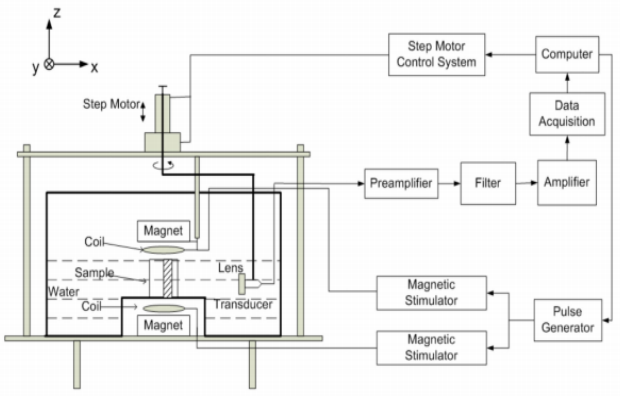


Fig. 2. MAT-MI Experimental Setup

Permanent magnets usually generate the static magnetic field to give a field strength of 0.1-0.3 Tesla in *z* direction around the sample [43], superconducting magnet is used with a 9.4 T MRI scanner, the imaging sample is rotating while the coil and transducer were fixed due to limited space in the MRI bore. For dynamic magnetic field generation, Computer controlled magnetic stimulators are used to drive the coil load around the sample. MAT-MI system which used pulse magnetic stimulations, high voltage and high current switches to control capacitor discharge through connected coil load have been used by magnetic stimulators. High voltage capacitors that charged up to 600v is proposed in [25], While [34] use as high as 24kv. The corresponding maximum dynamic magnetic field, which can be measured by small sensing coils around the imaging object, ranged from 0.00125 T to 0.07 T [45]. Magnetic stimulations sent through different coils have also been explored in the past but most MAT-MI system used a single magnetic stimulation generated through one coil set, such as a Helmholtz coil pair, which produces a region with a nearly uniform magnetic field [35]. In addition, MAT-MI systems using different coil sets to generate different magnetic stimulations and consequently different eddy current pattern in the conductive tissue sample have also been developed in the so-called multi-excitation MAT-MI system [46].

Ultrasound transducer mounted in certain scanning system that can either rotate the transducer or the imaging sample can be used to acquire MAT-MI signals around the imaging sample. Signal detected by the transducer are then filtered, amplified and fed to the data acquisition system. In MAT-MI, the magnetic induced eddy current in conductive tissues and the Lorentz force induced acoustic source are intrinsically distributed in the three-dimensional (3D) tissue volume. Induced force acoustic source is needed to map the 3D electrical conductivity distribution. Three-dimensional MAT-MI systems have been previously developed based on ultrasound focusing and cylindrical scanning [47]. As shown in Fig. 2, through ultrasound focusing in the *Z* direction, we can localize the MAT-MI acoustic sources in a specific *XY* plane. A 2-dimensional (2D) MAT-MI image can be obtained at each cross section of the 3D object and vertical scans in the *Z* direction can provide a stack of 2D images, thus forming a 3D volume image of the object. With such a circular scan, the spatial resolution of the MAT-MI image in each slice is mainly determined by the central frequency and bandwidth of the transducer, while the resolution in *Z* direction is determined by the focusing beam width. For imaging objects that are uniform in the *Z* direction and with homogeneous static and dynamic magnetic field, the whole MAT-MI system can be simplified as a 2D system, in which only 2D ultrasound scan is needed [48,49]. For 2D ultrasound scans, besides the circular scan mode with large scanning radius around the objects using unfocused transducer, scanning in *B*-mode scan using focused transducer may also be used [50].

[4] CHALLENGES AND FUTURE DIRECTIONS

In spite of many technical advances achieved in these years on MAT-MI, limitations still exist in currently available MAT-MI methods in the aspects of dynamic magnetic stimulation, instrumentation and reconstruction algorithms and further improvement is necessary to make it useful and applicable in clinical setup.

4.1 Dynamic Magnetic Stimulation

With the use of solid-state high voltage and high current switch, the dynamic magnetic stimulation used in MAT-MI system has been substantially improved to about 0.07T in its maximum dynamic range. There may be some space of improvement in terms of the magnetic stimulations. Note here that with the increased magnetic stimulation strength, the assumption $B_1 << B_0$ may need to be modified to include the contribution of $J \times B_1$ in the induced Lorentz Force. MAT-MI imaging speed may be further improved by using electrically controlled ultrasound phased array instead of single element transducer and mechanical scanning.

4.2 Instrumentation

Another technical challenge in MAT-MI instrumentation is the electromagnetic interference (EMI) caused by the time varying magnetic field on the ultrasound transducer. Related to the turn off transients in the stimulator and the impulse response of the transducer, such EMI usually contaminates the MAT-MI signal for substantial long period (tens of μs) and have been observed to have some low frequency variations. Therefore, further band-pass filtering is usually needed before MAT-MI image reconstruction. Better ways to avoid the EM contamination to the ultrasound transducer, such as better EM shielding or the use of optical fiber based transducers may be further explored to allow acquiring ultrasound signals in a closer distance (e.g. when using transducer with shorter focus) and further improve the MAT-MI signal quality.

4.3 Reconstruction Algorithm

For electrical conductivity reconstruction through mapping MAT-MI acoustic sources such as the multi-excitation MAT-MI method, more sophisticated coil pattern designs may help better improve the inverse conditions and

the final image quality. On the other hand, the recently developed beam-forming current density vector source method has shown great potential for electrical conductivity reconstruction with the use of only single magnetic excitation. Ultrasound bandwidth limitations have been successfully tackled using inverse filtering in that method. Further improvement may be achieved by considering the conductivity gradient term using iterative process when calculating the electrical conductivity from the estimated current density vector.

4.4 MAT-MI in Clinical Application

In vitro or in vivo, animal experiments need to be further conducted to assess the MAT-MI method for high-resolution conductivity imaging. Different types of soft tissues, organs or the whole body may be explored in the future imaging studies. The most possible clinical application of MAT-MI is believed to be tumor detection especially in cancer screening and detection.

A recent work on magneto acoustic tomography with the aid of magnetic nanoparticles suggested such possibility; employing the magnetomotive force, magneto acoustic tomography in a MAT-MI compatible setup was demonstrated as a high-spatial-resolution approach to reconstruct the in vivo distributions of nanoparticles, and to further highlight tumor by a high contrast [51].

[5] CONCLUSION

This report reviews fundamental ideas of MAT-MI and major techniques developed in recent years. First, the physical mechanisms underlying MAT-MI imaging are described including the magnetic induction and Lorentz force induced acoustic wave propagation. Also, experimental setups and various imaging strategies for MAT-MI are reviewed and compared together with the corresponding experimental results. Finally, some of the existing challenges and future directions for MAT-MI research have been highlighted. With all the reported and future technical advancement, MAT-MI has the potential to become an important noninvasive modality for electrical conductivity imaging of biological tissue.

REFERENCES

[1] S.C. Qun Zhang, Multiphysics Modeling: Numerical Methods and Engineering Applications. United States of America: Tsinghua University Press Limited. Published by Elsevier Inc. 2016.

[2] A. Isselmou, G. Xu, S. Zhang, S. Saminu, I. Javaid, I. S. Ahmad, "Differential Deep Convolutional Neural Network Model for Brain Tumor Classification," Brain Sci. 11(3), 2021, 352.

[3] T. Widlak, O. S. "Hybrid tomography for conductivity imaging," physics.med-ph, 2011, 32.

[4] A. Isselmou, G. Xu, S. Zhang, S. Saminu, "Modified Self-Organizing Map Algorithm for Brain Tumor Detection and Analysis Using Magnetic Resonance Brain Images," Journal of Biomedical Engineering and Medical Imaging (6)2, 2019.

[5] X. Li, S. Hu, L. Li, S. Zhu, "Numerical study of magnetoacoustic signal generation with magnetic induction based on inhomogeneous conductivity anisotropy," Comput Math Methods Med. 2013; 2013:161357.

[6] A. Isselmou, G. Xu, S. Zhang, S. Saminu, I. Javaid, I. S. Ahmad "Brain Tumor identification by Convolution Neural Network with Fuzzy C-mean Model Using MR Brain Images." International Journal of Circuits, Systems and Signal Processing, 14, 2020, pp. 1096-1102.

[7] R.J. Sadleir, V. T. "Transcranial direct current stimulation (tDCS) in a realistic head model," Neuroimage, 51, 2010, pp. 1310–8.

[8] X. Li, K. Yu, B. He, "Magnetoacoustic tomography with magnetic induction (MAT-MI) for imaging electrical conductivity of biological tissue: a tutorial review," Physics in Medicine & Biology, 61, 2016, pp. 249–270.

[9] A. Isselmou, G. Xu, S. Zhang, S. Saminu, I. Javaid, "Deep Learning Algorithm for Brain Tumor Detection and Analysis Using MR Brain Images," ICIMH 2019, Ningbo, China,2019, pp. 28-32.

[10] S. Mandija, Non-Invasive Characterization of Brain Tissue Electrical Properties with MRI, PhD thesis, Utrecht University, the Netherlands, 2018

[11] A. Isselmou, G. Xu, S. Zhang, S. Saminu, "Brain Tumor Detection and Classification by Hybrid CNN-DWA Model Using MR Images. Current Medical Imaging," 17(1), 2021, pp. 1096-1102.

[12] P. Grasland-Mongrain, J.M. Mari, J.Y. Chapelon, C. Lafon, "Lorentz force electrical impedance tomography," Irbm. 34 ,2013, pp. 357–60.

[13] P. Grasland-Mongrain, F. Destrempes, J.M. Mari, R. Souchon, S. Catheline, J.Y. Chapelon, et al. "Acousto-electrical speckle pattern in Lorentz force electrical impedance tomography," Phys Med Biol., 60, 2015, pp. 3747–57.

[14] J.K. Seo, E.J. Woo, "Electrical tissue property imaging at low frequency using MREIT," IEEE Trans. Biomed Eng. 61, 2014, pp. 1390–9.

[15] L. Guo, G. Liu, H. Xia, "Magneto-Acousto-Electrical Tomography With Magnetic Induction for Conductivity Reconstruction," IEEE Trans Biomed Eng. 62, 2015, pp. 2114–24.

[16] L. Ke, W. Zu, Q. Du, J. Chen, X. Ding, "A bio-impedance quantitative method based on magnetic induction tomography for intracranial hematoma," Med. Biol. Eng. Comput. 58, 2020, pp. 857–869.

[17] L. Wang, H. Xia, G. Li, "Influence of transducer aperture on magnetoacoustic tomography resolution," In Proceedings of the 2020 12th International Conference on Bioinformatics and Biomedical Technology, Xi'an, China, 2020, pp. 22–24.

[18] L. Wang, G. Liu, "Novel reconstruction algorithm of magnetoacoustic tomography based on ring transducer array for acoustic speed inhomogeneous tissues," Med. Phys. 47, 2020, pp. 3533–3544.

[19] S.G. Wang, S.Q. Zhang, R. Ma, T. Yin, Z.P. Liu, "A study of acoustic source generation mechanism of Magnetoacoustic Tomograph,". Comput Med Imag Grap. 38, 2014, pp. 42–8.

[20] P. Grasland-Mongrain, R. Souchon, F. Cartellier, A. Zorgani, J.Y. Chapelon, C. Lafon, S. Catheline, "Imaging of Shear Waves Induced by Lorentz Force in Soft Tissues," Phys Rev Lett. 2014; 113

[21] L. Kunyansky, "A mathematical model and inversion procedure for magneto-acousto-electric tomography," Inverse Probl. 2012; 28.

[22] H. Xia, G. Liu, X. Huang, L. Guo, Y. Yang, and M. Lu, "The Forward and Inverse Problem Based on Magneto-Acoustic Tomography with Current Injection," Journal of Biomedical Science and Engineering, 10, 2017, pp. 97-105.

[23] L. Kunyansky, C.P. Ingram, R.S. Witte, "Rotational magneto-acoustic-electric tomography (MAET): Theory and experimental validation," Phys. Med. Biol. 62, 2017, pp. 3025–3050.

[24] X. Sun, D. Fang, D. Zhang, Q. Ma, "Acoustic dipole radiation based electrical impedance contrast imaging approach of magnetoacoustic tomography with magnetic induction," Med Phys., 40, 2013, 052902.

[25] L. Zhou, X. Li, S. Zhu, B. He, "Magnetoacoustic tomography with magnetic induction (MAT-MI] for breast tumor imaging: numerical modeling and simulation," Phys Med Biol. 56, 2011, pp. 1967–83.

[26] H. Ammari, S. Boulmier, and P. Millien, "A Mathematical and Numerical Framework for Magnetoacoustic Tomography with Magnetic Induction," Journal of Differential Equations, 259, 2015, pp. 5379-5405.

[27] R. Xia, X. Li, B. He, "Comparison study of three different image reconstruction algorithms for MAT-MI," IEEE Trans Biomed Eng. 57, 2010, pp. 708–13.

[28] X.D. Sun, F. Zhang, Q.Y. Ma, J. Tu, D. Zhang, "Acoustic dipole radiation based conductivity image reconstruction for magnetoacoustic tomography with magnetic induction," Applied Physics Letters. 2012, 100

[29] L. Zhou, S. Zhu, B. He, "A reconstruction algorithm of magnetoacoustic tomography with magnetic induction for an acoustically inhomogeneous tissue," IEEE Trans Biomed Eng. 61, 2014, pp. 1739–46.

[30] A.R. Zywica, "Magnetoacoustic tomography with magnetic induction for biological tissue imaging: numerical modelling and simulations,"

Archives of Electrical Engineering, 65(1), 2015, pp. 141–150.

[31] A.R. Żywica, "Magnetoacoustic Tomography with Magnetic Induction for Biological Tissue Imaging: Numerical Modelling and Simulations," Archives of Electrical Engineering, 65(1), 2016, pp. 141-150.

[32] X. Shi, G. Liu, X. Yan, Y. Li, "Simulation research on magneto-acoustic concentration tomography of magnetic nanoparticles with magnetic induction," Comput Biol Med. 2020, 119:103653.

[33] A. R. Zywica, M. Ziolkowski and S. Gratkowski, "Detailed Analytical Approach to Solve the Magnetoacoustic Tomography with Magnetic Induction (MAT-MI) Problem for Three-Layer Objects," Energies, 13, 2020, 6515.

[34] R. Ma, M. Yang, S. Zhang, X. Zhou, T. Yin, "Analysis of the singular values for conductivity reconstruction in magnetoacoustic tomography with magnetic induction," IEEE Access, 8, 2020, pp. 51753–51760.

[35] L. Mariappan, B. He, "Magnetoacoustic tomography with magnetic induction: bioimepedance reconstruction through vector source imaging," IEEE Trans Med Imaging. 32, 2013, pp. 619–27.

[36] M. Dai, X. Chen, T. Sun, L. Yu, M. Chen, H. Lin, S. Chen, "A 2D magneto-acousto-electrical tomography method to detect conductivity variation using multifocus image method. Sensors, 18, 2018, 2373.

[37] I. Hidayat, I.; I.D. Darpita, I. D.; S.K. Wijaya, S. K.; P. Prajitno, P. (2019). "The development of magnetoacoustic tomography system with current injection," Proceedings of the 4th International Symposium on Current Progress in Mathematics and Sciences (iscpms2018) - Depok, Indonesia, 2018, 2168, 020016.

[38] M. Ziolkowski, S. Gratkowski, A.R. Zywica, "Analytical and numerical models of the magnetoacoustic tomography with magnetic induction," COMPEL Int. J. Comput. Math. Electr. Electron. Eng. 37, 2018, pp. 538–548

[39] A.R. Zywica, M. Ziolkowski, S. Gratkowski, "Transient Lorentz force density distribution in a single and double layer conducting spheres," In Proceedings of the International Interdisciplinary PhD Workshop (IIPhDW), Swinouj´scie, Poland, 2018.

[40] X.H. Yan, Y. Zhang, G.Q. Liu, "Simulation research on effect of magnetic nanoparticles on physical process of magneto–acoustic tomography with magnetic induction," Chin. Phys. B, 27, 2018, 104302

[41] Z. Yu, S. Dai, Q. Ma, G. Guo, J. Tu and D. Zhang, "Conductivity Anisotropy Influence on Acoustic Sources for Magnetoacoustic Tomography with Magnetic Induction," IEEE Transactions on Biomedical Engineering, doi:10.1109/TBME.2018.2805697

[42] S. Zhen, M. Zhen, "Numerical simulation of endoscopic magnetoacoustic tomography with magnetic induction." Comput. Biol. Med., 90, 2017, pp. 1–14.

[43] L. Mariappan, Q. Shao, C. Jiang, K. Yu, S. Ashkenazi, J.C. Bischof, B. He, "Magneto acoustic tomography with short pulsed magnetic field for in-vivo imaging of magnetic iron oxide nanoparticles," Nanomedicine. 12, 2016, pp. 689–99.

[44] L. Mariappan, G. Hu, B. He, "Magnetoacoustic tomography with magnetic induction for high-resolution bioimepedance imaging through vector source reconstruction under the static field of MRI magnet," Med Phys. 41, 2014, 022902.

[45] X.D. Sun, X. Wang, Y.Q. Zhou, Q.Y. Ma, and D. Zhang, "Reception pattern influence on magnetoacoustic tomography with magnetic induction," Chinese Physics B, 24(1), 2015, pp. 1-9.

[46] X. Li, B. He, "Multi-excitation magnetoacoustic tomography with magnetic induction for bioimpedance imaging," IEEE Trans Med Imaging. 29, 2010, pp. 1759–67.

[47] Z. Wei et al. "Image Reconstruction in Magnetoacoustic Tomography with Magnetic Induction With Variable Sound Speeds," IEEE Trans. Biomed. Eng., 63(12), 2016, pp. 2585-2594.

[48] G. Guo,Y. Gao,Y. Li et al., "Second harmonic magnetoacoustic responses of magnetic nanoparticles in magnetoacoustic tomography with magnetic induction," [J]. Chin. Phys. B, 29(3), 2020, 034302.

[49] X. Yan, Y. Pan, Y. Zhang, S. Guang, "Simulation study on forward problem of magnetoacoustic tomography with magnetic induction based on nanoparticles," Prog. Electromangetics Res. Lett.87, 2019, pp. 75–80.

[50] Z. Yuqi, W. Jiawei, S. Xiaodong, M. Qingyu, Z. Dong, "Transducer selection and application in magnetoacoustic tomography with magnetic induction," Journal of Applied Physics, 119(9), 2016, 094903.

[51] X.H. Yan, Y. Zhang, G.Q. Liu, "Simulation research on effect of magnetic nanoparticles on physical process of magneto–acoustic tomography with magnetic induction," Chin. Phys. B, 27, 2018, 104302.